Inorganic Chemistry

Article

pubs.acs.org/IC

Zirconium Complexes of Phenylene-Bridged {ONSO} Ligands: Coordination Chemistry and Stereoselective Polymerization of *rac*-Lactide

Ayellet Stopper,[†] Konstantin Press,[†] Jun Okuda,[‡] Israel Goldberg,[†] and Moshe Kol*[,†]

[†]School of Chemistry, Raymond and Beverly Sackler Faculty of Exact Sciences, Tel Aviv University, Ramat Aviv, Tel Aviv 69978, Israel

[‡]Institute of Inorganic Chemistry, RWTH Aachen University, Landoltweg 1, D-52056 Aachen, Germany

Supporting Information

ABSTRACT: Sequential tetradentate dianionic thio-imine diphenolate ligands featuring an *ortho*-phenylene core and their zirconium complexes are described for the first time. Ligands that include different combinations of bulky-alkyl groups and halo groups on the two phenol arms were prepared by a substitution/condensation reaction sequence. An unexpected *fac-fac* wrapping mode was found in the solid state for the ligands in the octahedral [{ONSO}Zr(O^tBu)$_2$] complexes. The complexes were all fluxional, and the barrier for enantiomer interconversion was found to depend on the phenolate substituents. The complexes were found to catalyze the polymerization of *rac*-lactide to poly(lactic acid) in solution with polymer tacticities varying from heterotactic to atactic which showed correlation to the nature of phenolate substituents but not to the degree of complex fluxionality.

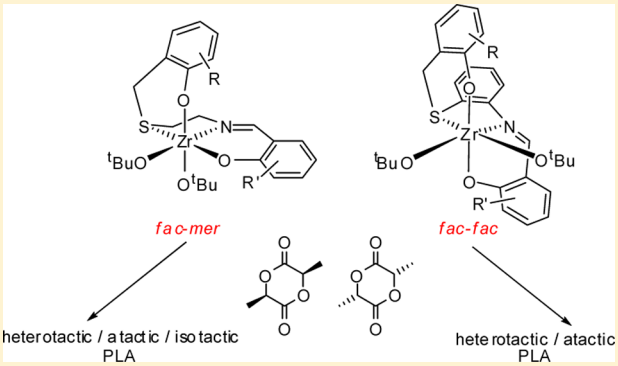

INTRODUCTION

Poly(lactic acid), PLA, is a biodegradable polyester that may be produced from annually renewable resources like corn and is therefore attracting considerable attention as a possible substitute for traditional polymers like polystyrene in packing applications.[1,2] In addition, its biocompatibility renders it suitable for biomedical applications which include bioresorbable sutures and stents.[3] The most convenient method of producing PLA is the catalytic ring opening polymerization (ROP) of the strained cyclic diester lactide (LA).[4] Lactide includes two stereogenic centers giving rise to three stereoisomers: (*S*,*S*)-L-lactide, (*R*,*R*)-D-lactide, and *meso*-lactide. The ROP does not involve formation of new stereogenic centers or epimerization of existing ones, except when strongly basic catalysts are employed. Therefore, the homochiral L-lactide or D-lactide lead to the isotactic polymers PLLA and PDLA, respectively. Polymerization of *rac*-LA can lead to the stereoregular microstructures: isotactic diblock (by a site control mechanism operating for enantiomerically pure catalysts),[5] isotactic multiblock (by a chain-end control mechanism[6] or site control mechanism combined with polymeryl exchange operating for racemic catalysts[7]), as well as the gradient isotactic multiblock[8] (by the combined action of site control and chain end control mechanisms[9]) or heterotactic (by either a chain-end control mechanism or, presumably, a site control mechanism combined with alternating catalyst enantiomer interconversion)[10,11] as well as to the stereoirregular atactic PLA. The different PLA microstructures affect the physical properties of the polymer including its melting point and rate of hydrolysis, and so, controlling the type and degree of polymer tacticity by catalyst design has been attracting considerable attention in the past 15 years.[12]

Most of the catalyst systems that were introduced in that period are heteroleptic complexes of various metals, including aluminum, zinc, and yttrium. Complexes of group 4 transition metals have been attracting growing attention in recent years.[13] In particular, well-defined complexes of tetradentate ligands were shown to lead to desired catalyst properties including high activity and high degree of stereocontrol. These ligands typically rely on phenolate, alcoholate or related anionic donors and neutral amine or thio donors.[10j,11e−g,14] Structure−activity relationship studies have shown that the metal employed, the coordination number of the complex, the ligand wrapping mode tendency and symmetry of the complex, the nature and location of substituents in the chelating ligand backbone, and the rigidity/fluxionality of the complex may all affect the activity and the type and degree of stereoselectivity of the catalyst. For example, halo-phenolate substituents in amine bis(phenolate) complexes led to increased activity in comparison to bulky-alkyl substituents,[14a] amine tris(phenolate) complexes of zirconium and hafnium catalyzed

Received: May 19, 2014
Published: August 14, 2014

   dx.doi.org/10.1021/ic501164c | *Inorg. Chem.* 2014, 53, 9140−9150

the polymerization of *rac*-lactide to heterotactic PLA while the respective titanium complex led to atactic PLA,[11e] and fluxional dithiodiolate as well as phenylenediamine diphenolate group 4 complexes exhibited exceptional catalytic activities and high heteroselectivities.[11f,g]

Recently, we introduced the tetradentate-dianionic imine-thiobis(phenolate) {ONSO}-type ligands, and their group 4 metal complexes.[15] These ligands were designed to include a rigid imine-donor expected to orient its two adjacent donors in a *meridional* manner and a fluxional thio-donor expected to orient its two adjacent donors in a *facial* manner. Altogether, semifluxional *fac-mer* octahedral complexes of group 4 metals were proposed to result. The zirconium complexes of these {ONSO} ligands were found to feature a dynamic behavior in which two C_1-symmetric enantiomers were equilibrating to C_s-averaged species. The barrier to enantiomer interconversion in these complexes was found to depend on the bulk of the substituents on the two phenol rings. Significantly, bulkier phenol substituents on the supposedly more flexible {OSN}-segment of the molecule were found to have a more pronounced effect on the barrier of interconversion relative to the same phenol substituents when placed on the supposedly more rigid {ONS}-segment of the molecule. While these findings supported the proposed *fac-mer* ligand wrapping (Figure 1), crystallographic evidence was lacking. These

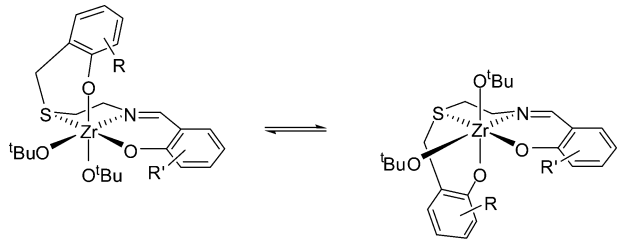

Figure 1. Inversion of proposed *fac-mer* ethylene-bridged {ONSO}-Zr complexes. R substituents have a stronger effect on interconversion barrier height than R′ substituents.

complexes were found to catalyze the polymerization of *rac*-lactide to PLA whose type of tacticity and its degree roughly correlated with the degree of complex fluxionality: the most fluxional complexes led to heterotactically inclined PLA, the most rigid complexes led to isotactically inclined PLA, and the complexes in between led to atactic PLA.[16] These intriguing results prompted us to further explore structure−activity relationships in this family of ligands. Herein we introduce a new variety of this imine-thiobis(phenolate) {ONSO}-type ligands that includes a central phenylene unit rather than the prototypical ethylene unit described above. We show that these new tetradentate ligands wrap stereoselectively, yet in an unexpected wrapping mode around zirconium, and describe their dynamic behavior and their catalytic activity and stereocontrol in polymerization of *rac*-lactide.

RESULTS AND DISCUSSION

Ligands Design and Synthesis. The phenylene-bridged {ONSO} ligand precursors described in the current work are outlined in Scheme 1. Since the tetradentate {ONSO} ligands are nonsymmetric, given substituents may play different roles depending on which of the two phenolate rings they are positioned. To address structural and dynamic parameters and deduce structure−activity relationships they were designed to include different combinations of electron withdrawing halo groups of different bulk (Cl and Br) and bulky alkyl groups (*tert*-butyl and 1-adamantyl) on either of the two phenol arms. Ligand precursors $Lig^{1-4}H_2$ include all possible combinations of *ortho,para*-dichloro and *ortho,para*-dibromo substituents on the two phenol arms. Ligand precursors $Lig^{5,6}H_2$ include the combinations of dichlorophenolate and di-*tert*-butyl phenolate and $Lig^{7,8}H_2$ include the combinations of dichlorophenolate and *ortho*-1-adamantyl-*para*-methyl phenolate. Our preliminary synthetic attempts included condensation of a substituted salicylaldehyde with the amine group of 2-aminothiophenol followed by nucleophilic reaction of the thio group with a substituted 2-(bromomethyl)phenol, in analogy to the synthesis of the ethylene-bridged {ONSO} ligands. However, this route led to the target ligands in very low yields. We therefore attempted the reverse route, viz. starting with the nucleophilic thio-substitution and following with the amine-condensation which resulted in improved overall yields of 30−100% (Scheme 1). In all cases, the first reaction step yielded the thio-substituted intermediate in quantitative yields consistent with the higher nucleophilicity of the thio group relative to that of the aromatic amine group. The attempted synthesis of phenylene-{ONSO} ligands that include bulky alkyl groups on both of the phenol arms by any of the reaction sequences did not lead to sufficient quantities of ligands for further complexation studies.

Synthesis of Zirconium Complexes. Reaction of the ligand precursors $Lig^{1-4}H_2$ that include different combinations of halo-substituents on the two phenol rings with one molar equivalent of $Zr(O^tBu)_4$ in diethyl ether gave the desired

Scheme 1. Synthesis and Variety of the Phenylene-{ONSO} Ligand Precursors

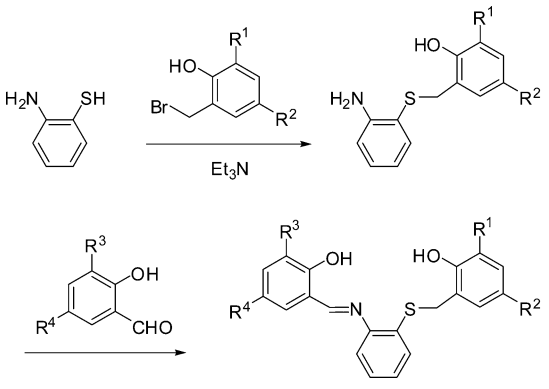

Lig^1H_2: $R^1 = R^2 = R^3 = R^4 = Cl$
Lig^2H_2: $R^1 = R^2 = R^3 = R^4 = Br$
Lig^3H_2: $R^1 = R^2 = Cl$, $R^3 = R^4 = Br$
Lig^4H_2: $R^1 = R^2 = Br$, $R^3 = R^4 = Cl$
Lig^5H_2: $R^1 = R^2 = Cl$, $R^3 = R^4 = {}^tBu$
Lig^6H_2: $R^1 = R^2 = {}^tBu$, $R^3 = R^4 = Cl$
Lig^7H_2: $R^1 = R^2 = Cl$, $R^3 = Ad$, $R^4 = Me$
Lig^8H_2: $R^1 = Ad$, $R^2 = Me$, $R^3 = R^4 = Cl$

dx.doi.org/10.1021/ic501164c | Inorg. Chem. 2014, 53, 9140−9150

complexes of the form $Lig^{1-4}Zr(O^tBu)_2$. However, in all cases, the formation of these complexes was accompanied by formation of the homoleptic complexes $(Lig^{1-4})_2Zr$ (which lack monodentate labile alkoxo groups) as side-products in up to 1:1 ratio (Scheme 2). Attempts to avoid the formation of the

Scheme 2

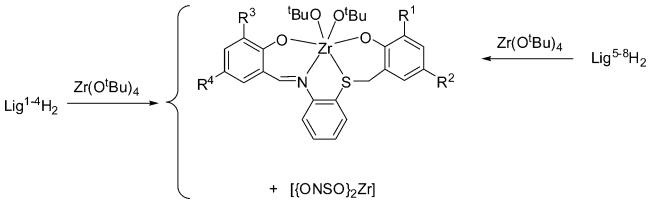

homoleptic complexes by reversing the order of addition of reactants or changing their molar ratio, as well as changing the solvent (pentane or toluene) or lowering the reaction temperature were unsuccessful. The homoleptic complexes $(Lig^{1-4})_2Zr$ could be prepared in pure form by reacting the ligand precursors with $Zr(O^tBu)_4$ in a 2:1 molar ratio. The ^1H NMR spectra of the homoleptic complexes are consistent with C_2-symmetric species which are rigid according to VT-NMR experiments. Comproportionation reaction attempts between the homoleptic complexes and $Zr(O^tBu)_4$ did not lead to the $Lig^{1-4}Zr(O^tBu)_2$–type complexes. The separation of the target $(Lig^{1-4})Zr(O^tBu)_2$ complexes from the homoleptic complexes proved challenging and took advantage of the higher solubility of the former in pentane. Thus, filtration off of the precipitated homoleptic complexes from the ethereal reaction mixture, removal of the ether under vacuum, extractions with pentane and further removal of the slowly precipitating homoleptic complex, and finally crystallization from pentane gave the target complexes in low to medium isolated yields. This procedure was successful for complexes $Lig^{2-4}Zr(O^tBu)_2$ while the full removal of the homoleptic complex $(Lig^1)_2Zr$ to give substantial quantities of complex $Lig^1Zr(O^tBu)_2$ (beyond crystals suitable for diffraction analysis; see below) was not accomplished to date and the latter was obtained in a maximum purity of *ca.* 85%. We found that the homoleptic complexes were inactive in polymerization of *rac*-lactide, so they could be regarded as inert impurities. On the other hand, the ligand precursors $Lig^{5-8}H_2$ reacted with one molar equivalent of $Zr(O^tBu)_4$ and led to the desired zirconium complexes $Lig^{5-8}Zr(O^tBu)_2$ with no contamination of the homoleptic complexes. We attribute this difference to the increased steric bulk of the tertiary alkyl phenolate substituents, which would have led to excessive crowdedness if homoleptic complexes were to form.

Dynamic Behavior of the Zirconium Complexes. Except for the *mer-mer* wrapping mode which gives the *trans* stereoisomer, all the other wrapping modes of sequential nonsymmetric tetradentate ligands around octahedral complexes of the type $[LigZr(O^tBu)_2]$ (*fac-fac*; *fac-mer*; *mer-fac*) give chiral C_1-symmetric *cis* stereoisomers.[17] We found that all the zirconium complexes of the type $[\{ONSO\}Zr(O^tBu)_2]$ were fluxional and that their barriers for enantiomer interconversion were proportional to the bulk of the substituents on both of the phenolate rings. The complexes $[Lig^{1-4}Zr(O^tBu)_2]$ featuring only halo phenolate substituents appeared C_s-symmetric at RT consistent with a fast exchange regime whereas complexes $[Lig^{5-8}Zr(O^tBu)_2]$ featuring a combination of halo and bulky-alkyl substituents appeared C_1-symmetric at RT consistent with a slow exchange regime. Line shape analysis of the ^1H NMR spectra of the zirconium complexes in d_8-toluene measured at variable temperatures revealed barriers of $\Delta G^{\ddagger}$ = 13.0(1.5), 14.6(1.0), 13.8(0.5), 14.2(0.4) kcal mol^{-1} for $Lig^{1-4}Zr(O^tBu)_2$, respectively, and $\Delta G^{\ddagger}$ = 16.1(0.5), 17.6(0.3), 18.1(0.5), 17.9(0.5) kcal mol^{-1} for $Lig^{5-8}Zr(O^tBu)_2$, respectively (see Figure 2).

The interconversion barriers for the analogous "semi-rigid" ethylene-bridged {ONSO}-zirconium complexes that included combined bulky alkyl/halo substituents tended to be slightly lower on average (Figure 2).[15] We found some significant differences between these two series of complexes. For the ethylene-bridged {ONSO}-zirconium complexes higher barriers for enantiomer interconversion were found when the bulkier group was placed on the supposedly more fluxional part of the complex, namely on the phenolate proximal to the thio-donor. For example, a difference of 2.3 kcal mol^{-1} was recorded for the zirconium complexes of the two isomeric ligands featuring *tert*-butyl/chloro substituents and 3.4 kcal mol^{-1} for the zirconium complexes of the two isomeric ligands featuring adamantyl/chloro substituents (Figure 3, left). In contrast, for the complexes of the phenylene-bridged {ONSO} ligands described currently, the difference in barrier height was reduced

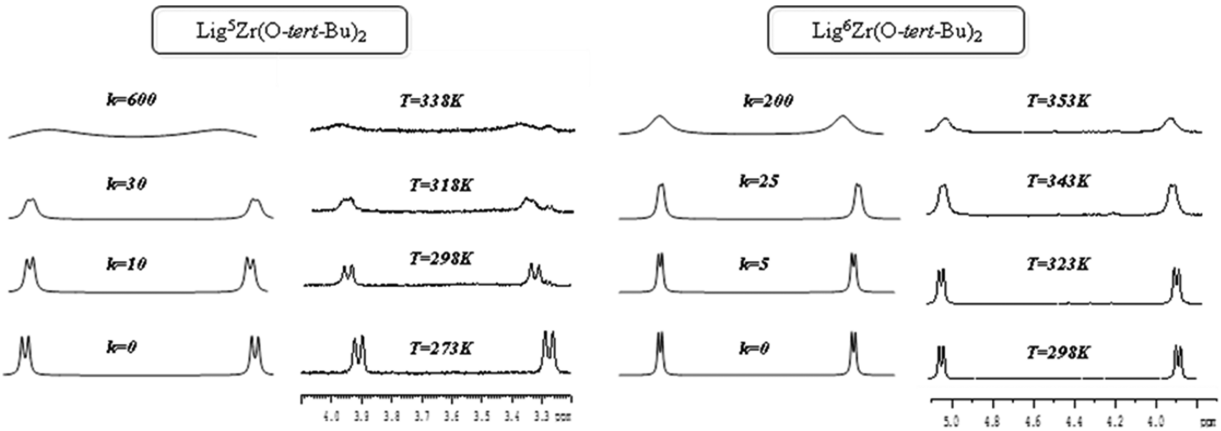

Figure 2. Methylene section of the ^1H NMR spectra taken at different temperatures of $Lig^5Zr(O^tBu)_2$ ($\Delta G^{\ddagger}$ = 16.1(0.5) kcal mol^{-1}) and $Lig^6Zr(O^tBu)_2$ ($\Delta G^{\ddagger}$ = 17.6(0.3) kcal mol^{-1}).

dx.doi.org/10.1021/ic501164c | Inorg. Chem. 2014, 53, 9140−9150

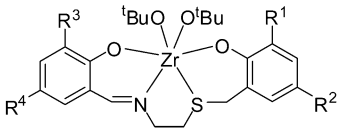

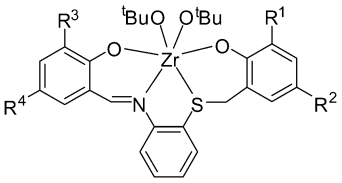

$R^1 = R^2 = Cl$, $R^3 = R^4 = {}^tBu$: $\Delta G^{\ddagger} = 13.3$ kcal/mol

$R^1 = R^2 = {}^tBu$, $R^3 = R^4 = Cl$: $\Delta G^{\ddagger} = 15.6$ kcal/mol

$R^1 = R^2 = Cl$, $R^3 = Ad$, $R^4 = Me$: $\Delta G^{\ddagger} = 15.5$ kcal/mol

$R^1 = Ad$, $R^2 = Me$, $R^3 = R^4 = Cl$: $\Delta G^{\ddagger} = 18.9$ kcal/mol

$[Lig^5Zr(Ot\text{-}Bu)_2]$: $\Delta G^{\ddagger} = 16.1$ kcal/mol

$[Lig^6Zr(Ot\text{-}Bu)_2]$: $\Delta G^{\ddagger} = 17.6$ kcal/mol

$[Lig^7Zr(Ot\text{-}Bu)_2]$: $\Delta G^{\ddagger} = 18.1$ kcal/mol

$[Lig^8Zr(Ot\text{-}Bu)_2]$: $\Delta G^{\ddagger} = 17.9$ kcal/mol

Figure 3. Barriers for enantiomer interconversion for ethylene-bridged and phenylene-bridged {ONSO}-Zr complexes featuring equivalent phenolate substituents.

to 1.5 kcal mol^{-1} for the two isomeric ligands featuring *tert*-butyl/chloro substituents, and utterly vanished for the two isomeric ligands featuring adamantyl/chloro substituents (Figure 3, right). The barrier height difference between the most fluxional and the most rigid complexes for the ligands including alkyl/halo substituents was 6.6 kcal mol^{-1} for the ethylene-bridged {ONSO} complexes, but only 2.0 kcal mol^{-1} for phenylene-bridged {ONSO} complexes. The smaller roles played by the phenolate substituents on the dynamic behavior of the current complexes may imply that both the {OSN} and the {ONS} segments are fluxional.

Crystallographic Studies. Single crystals suitable for X-ray diffraction analysis of complexes $Lig^1Zr(O^tBu)_2$, $Lig^2Zr(O^tBu)_2$, $Lig^4Zr(O^tBu)_2$ and $Lig^6Zr(O^tBu)_2$ were grown and their structures were solved. The ORTEP representations of the molecular structures are shown in Figure 4, and selected bond lengths and angles are given in Table 1. The four heteroatoms of the {ONSO} ligands are bound to the metal, and, together with the two monodentate alcoholate groups, complete a roughly octahedral geometry. All ligands were found to wrap in the same manner around zirconium, with both the {ONS} donor-array and the {OSN} donor-array binding in a *facial* manner leading to an altogether *fac-fac* ligand wrapping. While the *fac*-wrapping around the thio-donor is predictable based on the narrow C−S−C bond angle and previous solid-state structures,[18] the *fac*-wrapping around the imine-donor is unusual when considering the wide C−N−C bond angle and the previous structures of group 4 metal complexes of related ligands such as Salen,[19] Salophen,[20] and Salalen.[17,21] The sum of angles around the imine donor in all the present {ONSO}Zr complexes was 359.9−360° consistent with the sp^2 hybridization of the imine group. On the other hand, the phenylene bridge is severely tilted toward the phenol group proximal to the thio-donor, caused by the narrow angles around this donor. We propose that this tilting facilitates the facial wrapping around the imine-donor. The fluxional behavior recorded for these complexes should thus equilibrate two *fac-fac* enantiomers (Figure 5), instead of two *fac-mer* enantiomers as previously proposed for the ethylene-bridged {ONSO}-complexes (Figure 1). The trend noted above, namely, the weak dependence of the barrier height on location of the two phenolate substituents is consistent with this *fac-fac* geometry in which both the {ONS} and the {OSN} segments of the molecule need to twist in order to reverse the overall chirality. Comparison of the bond lengths and angles in these structures reveals a few recurring structural themes. For all complexes, the Zr−O2 bond between the zirconium and the phenolate oxygen proximal to the thio donor is slightly shorter than the Zr−O3 bond between the zirconium and the phenolate oxygen proximal to the imine donor. This might be due to the different chelate-ring conformations, or due to weaker electron donation of O3 (which is strongly conjugated to the aromatic ring) to Zr. In addition, for all complexes, the Zr−O7 bonds are slightly longer than the Zr−O6 bonds, which may result from a stronger *trans*-influence of the imine-donor relative to the thio-donor. Very similar bond lengths and angles are found for $Lig^1Zr(O^tBu)_2$, $Lig^2Zr(O^tBu)_2$ and $Lig^4Zr(O^tBu)_2$ whose {ONSO} ligands include only halo-substituents. Some of these values, including the Zr−N bond, the Zr−O6 and Zr−O7

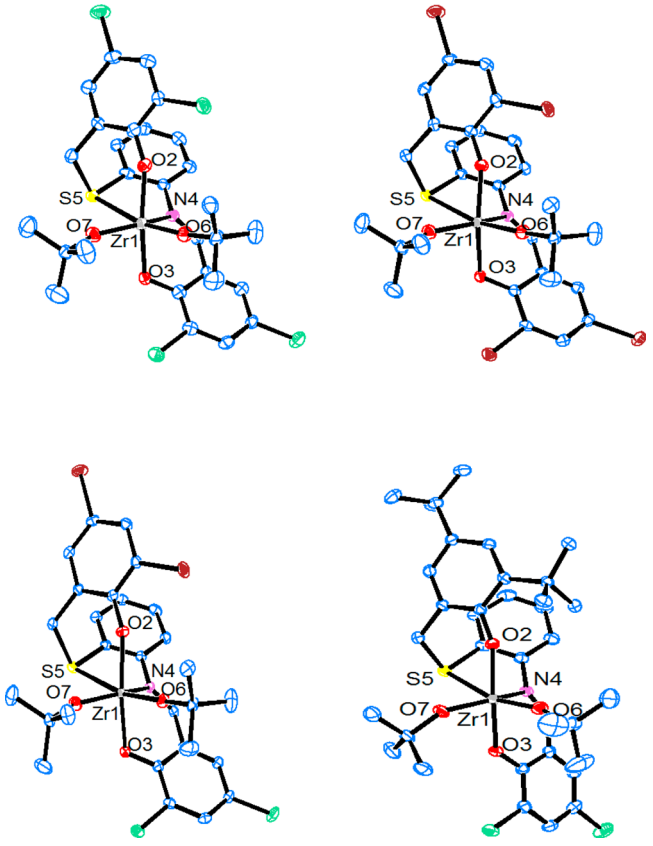

Figure 4. ORTEP representations of the molecular structures of $Lig^1Zr(O^tBu)_2$ (top left), $Lig^2Zr(O^tBu)_2$ (top right), $Lig^4Zr(O^tBu)_2$ (bottom left), and $Lig^6Zr(O^tBu)_2$ (bottom right).

dx.doi.org/10.1021/ic501164c | Inorg. Chem. 2014, 53, 9140−9150

Table 1. Selected Bond Lengths and Angles

	$Lig^1Zr(O\text{-}t\text{-}Bu)_2$	$Lig^2Zr(O\text{-}t\text{-}Bu)_2$	$Lig^4Zr(O\text{-}t\text{-}Bu)_2$	$Lig^6Zr(O\text{-}t\text{-}Bu)_2$
bond lengths				
Zr−O2	2.028(3)	2.0284(19)	2.0285(14)	2.0173(15)
Zr−O3	2.110(3)	2.1145(19)	2.1125(15)	2.1012(15)
Zr−N4	2.419(3)	2.420(2)	2.4181(17)	2.381(2)
Zr−S5	2.8636(12)	2.8866(7)	2.8950(6)	2.8655(7)
Zr−O6	1.897(3)	1.9025(18)	1.8986(14)	1.9130(18)
Zr−O7	1.914(3)	1.918(2)	1.9100(15)	1.9372(17)
bond angles				
O2−Zr−O3	158.26(11)	157.04(8)	157.36(6)	164.01(7)
O6−Zr−O7	108.50(13)	108.19(9)	108.08(7)	111.55(8)

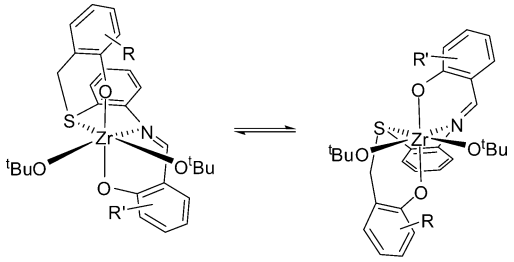

Figure 5. Inversion of *fac-fac* phenylene-bridged {ONSO}-Zr complexes. The differences between the influence of the R and R′ substituents on interconversion barriers height were found to be small.

bonds—the two bonds to the monodentate alkoxo bonds, and the O2−Zr−O3 angle are slightly different for $Lig^6Zr(O^tBu)_2$.

The unexpected *fac-fac* wrapping of the phenylene-bridged {ONSO} ligands around zirconium prompted us to gain further structural information on the group 4 complexes of the prototypical ethylene-bridged {ONSO} ligands, for which a *fac-mer* wrapping was proposed but had not been demonstrated crystallographically. Single crystals suitable for X-ray diffraction of a hafnium complex of the ethylene-bridged {ONSO} ligand featuring *tert*-butyl substituents on both phenolates − $[\{ONSO\}Hf(O^tBu)_2]$ were grown from a mixture of toluene and pentane at −35 °C and the structure was solved. The molecular structure of this complex and selected bond lengths and angles are given in Figure 6. Most notably, this ethylene-bridged ligand binds in the originally proposed *fac* ({OSN} fragment) *mer* ({ONS} fragment) mode. We suggest that this *fac-mer* wrapping mode is common to all ethylene-bridged {ONSO} octahedral complexes of group 4 metals. This wrapping supports the stronger influence of the thio-proximal phenolate substituents on the barrier to interconversion found for the complexes of these prototypical {ONSO} ligands. The *fac-mer* wrapping around group 4 metals is a characteristic of the {ONN′O} Salalen ligands.[17,21] Notably, the M-O bond of the monodentate alkoxo group *trans* to the neutral imine-donor was found to be shorter than the M-O bond of the monodentate alkoxo group *trans* to the anionic phenoxo-donor for the Salalen and the ethylene-bridged {ONSO} classes of complexes, consistent with the stronger *trans*-influence of the anionic donor relative to the neutral donor. The angle between the two labile alkoxo groups in these two types of complexes is very similar (ca. 98.5°), and is much narrower than the O6−Zr−O7 angles found for the *fac-fac* wrapping phenylene-bridged {ONSO} complexes noted above.

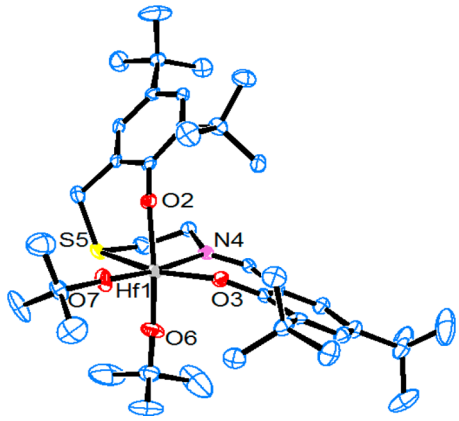

Figure 6. ORTEP representation of the molecular structure of the ethylene-bridged {ONSO} complex $[\{ONSO\}Hf(O\text{-}t\text{-}Bu)_2]$. Selected bond lengths (Å) and angles (deg): Hf O2 2.066(4), Hf O3 2.008(4), Hf N4 2.362(5), Hf S5 2.7173(16), Hf O6 1.932(4), Hf O7 1.917(4), O6 Hf O7 98.3(8).

Polymerization Studies. We studied the catalytic activity of the phenylene-bridged {ONSO} zirconium complexes in polymerization of racemic lactide (see Table 2). All complexes were found to be active when the polymerizations were conducted in toluene at 70 °C. Lower activities were recorded when THF was employed as solvent possibly due to competitive coordination (entry 2). The complexes including halo-only substituted {ONSO} ligands ($Lig^{1-4}Zr(O^tBu)_2$) exhibited higher activities, and consumed practically all of the 300 equiv of monomer within 4 h. The activity of the complexes including combinations of halo/alkyl substituted {ONSO} ligands ($Lig^{5-8}Zr(O^tBu)_2$) were lower and required longer times to reach high conversions (entries 6−10). Polymerizations at 50 °C were slower, and, in particular, $Lig^6Zr(O^tBu)_2$ and $Lig^8Zr(O^tBu)_2$ featuring bulky alkyl groups on the thio-side phenolate and chloro groups on the imine-side phenolate were practically inactive (entries 18, 20). In most cases, PLA samples having narrow molecular weight distributions were obtained supporting a controlled polymerization. In some cases PDI values lower than 1.10 were obtained. In most cases, the number-average molecular weight (M_n) of the obtained PLA samples was in close agreement with the theoretical value calculated from the number of consumed lactide equivalents. This implies that the complex molecules were fully activated, and that a single polymeryl chain grows on each metal center albeit the presence of two monodentate alkoxo-groups in the complexes.

The stereoregularity of the polymers ranged from heterotactic to atactic, depending on the structure of the catalyst and on the polymerization conditions. Complexes $Lig^{1-4}Zr(O^tBu)_2$ that feature halo substituents on both of the phenolate arms led to PLA of uniform heterotacticity values of P_r of ca. 0.75 at 70 °C which did not change upon changing the solvent to THF (entries 1−5). These catalysts were heterospecific at 50 °C as well, and a maximum heterotacticity of P_r = 0.87 was recorded for $Lig^4Zr(O^tBu)_2$. Complexes $Lig^{5-8}Zr(OtBu)_2$ that combine halo and alkyl phenolate substituents portrayed a more complex stereocontrol. Complexes $Lig^5Zr(OtBu)_2$ and $Lig^7Zr(OtBu)_2$ that include a bulky alkyl group on the imine-side phenol led to heterotactic PLA at 70 °C and at 50 °C (entries 6, 7, 9, 17, 19). On the other hand, complexes $Lig^6Zr(OtBu)_2$ and $Lig^8Zr(OtBu)_2$ that feature the opposite substitution pattern led to

dx.doi.org/10.1021/ic501164c | Inorg. Chem. 2014, 53, 9140−9150

Table 2. ROP of *rac*-Lactide

entry	initiator[a]	temp. (°C)	time (h)	conv.	M_w[b] (g mol^{-1})	M_n[b] (g mol^{-1})	PDI	$M_{n,calc}$[c] (g mol^{-1})	P_r[d]
1	Lig^{1}Zr(O^{t}Bu)$_2$	70	4	0.93	50,600	41,300	1.23	40,100	0.75
2[e]	Lig^{1}Zr(O^{t}Bu)$_2$	70	24	0.57	23,400	18,500	1.27	24,600	0.74
3	Lig^{2}Zr(O^{t}Bu)$_2$	70	4	0.97	61,600	48,600	1.26	41,900	0.78
4	Lig^{3}Zr(O^{t}Bu)$_2$	70	4	0.98	54,600	44,400	1.23	42,300	0.78
5	Lig^{4}Zr(O^{t}Bu)$_2$	70	4	0.90	81,800	70,800	1.15	38,800	0.76
6	Lig^{5}Zr(O^{t}Bu)$_2$	70	8	0.70	19,800	18,400	1.07	30,200	0.76
7	Lig^{5}Zr(O^{t}Bu)$_2$	70	20	1.0	49,000	36,100	1.36	43,200	0.76
8	Lig^{6}Zr(O^{t}Bu)$_2$	70	8	0.78	37,900	32,600	1.16	33,700	0.52
9	Lig^{7}Zr(O^{t}Bu)$_2$	70	24	0.53	19,700	14,200	1.38	22,900	0.70
10	Lig^{8}Zr(O^{t}Bu)$_2$	70	24	0.72	32,800	30,500	1.07	31,100	0.51
11	Lig^{1}Zr(O^{t}Bu)$_2$	50	6	0.85	33,500	30,900	1.08	36,700	0.81
12	Lig^{2}Zr(O^{t}Bu)$_2$	50	6	0.38	22,900	21,200	1.07	16,400	0.73
13	Lig^{2}Zr(O^{t}Bu)$_2$	50	67	1.0	49,400	44,000	1.12	43,200	0.73
14	Lig^{3}Zr(O^{t}Bu)$_2$	50	24	0.85	34,200	31,300	1.09	36,700	0.79
15	Lig^{4}Zr(O^{t}Bu)$_2$	50	6	0.57	30,100	26,700	1.12	24,600	0.87
16	Lig^{4}Zr(O^{t}Bu)$_2$	50	24	1.0	48,200	42,600	1.13	43,200	0.87
17	Lig^{5}Zr(O^{t}Bu)$_2$	50	72	0.65	24,600	23,300	1.06	28,000	0.78
18	Lig^{6}Zr(O^{t}Bu)$_2$	50	24	0					
19	Lig^{7}Zr(O^{t}Bu)$_2$	50	48	0.43	10,700	9,800	1.09	18,600	0.67
20	Lig^{8}Zr(O^{t}Bu)$_2$	50	24	0					

[a] 10 μmol of catalyst and 300 equiv of *rac*-LA in 5 mL toluene as solvent. [b] correction parameter: 0.58 × M_n polystyrene standards. [c] calculated from 144.13 × (LA/I) × conversion of monomer. [d] P_r is the probability for heterotactic enchainment calculated from homonuclear decoupled ^{1}H NMR spectrum. [e] 5 mL of THF was used as solvent.

practically atactic PLA at 70 °C (entries 8, 10, and were inactive at 50 °C). As noted above, the ethylene-bridged {ONSO} zirconium complexes polymerized *rac*-LA to give PLA with tacticities that ranged from heterotactic via atactic to isotactic. For those systems we found that the phenolate substitution pattern affected both the degree of complex fluxionality and the type and degree of PLA tacticity. Thus, we could not determine whether the tacticity was affected primarily by the substitution pattern or by the fluxionality of the catalyst. The current phenylene-bridged {ONSO} zirconium complexes feature a *fac-fac* ground state geometry whereas the ethylene-bridged {ONSO} zirconium complexes feature a *fac-mer* ground state geometry, yet some comparison between the two is of interest. For both families of complexes, the most fluxional member (Lig^{5}Zr(O^{t}Bu)$_2$ and its ethylene-bridged analogue) had the same phenolate-substitution pattern and led to the highest degrees of heterotacticity. However, while the rigidification of the ethylene-bridged {ONSO}-Zr systems led to a decrease in heterotacticity, such a correlation was not found for the current phenylene-bridged {ONSO}-Zr systems, and, in fact, the most rigid complex (Lig^{7}Zr(O^{t}Bu)$_2$) also led to heterotactic PLA. We conclude that, for the current catalysts, the type and degree of tacticity is better correlated with the phenolate substitution pattern than with the fluxionality of the complex. Alkyl-only substituted phenylene-bridged {ONSO} ligands are expected to lead to more rigid complexes and possibly to isotatic PLA, however, an efficient synthesis of these ligands was not achieved heretofore.

CONCLUSIONS

The phenylene-bridged tetradentate dianionic thio-imine diphenolate ligands were described for the first time, following a two-step "reverse" synthetic scheme. Ligands featuring various combinations of halo phenolate substituents as well as halo/bulky-alkyl phenolate substituents were prepared. The less bulky ligands reacted with tetra(*tert*-butoxy)zirconium to give mixtures of the desired octahedral complexes [{ONSO}Zr(O^{t}Bu)$_2$] and the bis-homoleptic complexes [{ONSO}$_2$Zr] while the more bulky ligands reacted with tetra(*tert*-butoxy) zirconium to give the desired complexes [{ONSO}Zr(O^{t}Bu)$_2$] exclusively. Single fluxional stereoisomers of the desired complexes were obtained in all cases, however, in contrast to the analogous ethylene-bridged {ONSO} ligands, the wrapping mode of the current ligands around the octahedral zirconium center was found to be *fac-fac*, and the barrier for enantiomer interconversion showed a weak dependence on the specific phenolate location of the substituents. All complexes were found to catalyze the polymerization of *rac*-LA to PLA in solution in a controlled fashion, and with stereocontrol that was derived from the ligand substitution pattern. All complexes of {ONSO} ligands that featured halo substituents on the thio-side phenolate led to heterotactic PLA, irrespective of the substituents on the imine-side phenolate, whereas complexes of {ONSO} ligands that featured bulky-alkyl substituents on the thio-side phenolate led to atactic PLA. On the other hand, no correlation was found between the fluxionality of the complexes and their stereocontrol in *rac*-LA polymerization. We are currently designing catalysts for stereoregular lactide polymerization based on the structure–activity relationships revealed herein.

EXPERIMENTAL SECTION

General. The handling of air-sensitive materials and the purification and drying of solvents was performed as previously described.[15] 3,5-dichloro-2-hydroxybenzaldehyde, 3,5-di-*tert*-butyl-2-hydroxybenzaldehyde, 2-Aminothiophenol, triethylamine, and Zr(*tert*-butoxide)$_4$ were purchased from Aldrich and used as received. *Rac*-lactide was prepared by mixing equal amounts of L-lactide and D-lactide (obtained from Purac) and was recrystallized from toluene. 3-adamantyl-2-hydroxy-5-methylbenzaldehyde,[22] 2-(bromomethyl)-4,6-dichlorophenol,[23] 2-(bromomethyl)-4,6-di-*tert*-butylphenol,[24] and 2-(bromomethyl)-4-methyl-6-adamanthylphenol[25] were synthesized according to published procedures.

dx.doi.org/10.1021/ic501164c | *Inorg. Chem.* 2014, 53, 9140–9150

NMR data acquisition, elemental analyses, and PLA molecular weight determination were performed according to previously published protocols.[15] X-ray diffraction measurements were performed on a Nonius Kappa CCD ($Lig^1Zr(O^tBu)_2$, $Lig^2Zr(O^tBu)_2$, and $Lig^6Zr(O^tBu)_2$) and Apex Duo (Bruker-AXS) ($Lig^4Zr(O^tBu)_2$, and [{ethylene-ONSO}Hf(O-*t*-Bu)$_2$]) diffractometer systems using Mo Kα (λ = 0.7107 Å) radiation. The analyzed crystals were embedded within a drop of viscous oil and freeze-cooled to ca. 110 K.

Synthesis of 2-((2-aminothiophenyl)methyl)-4,6-dichlorophenol. A solution of 2-(bromomethyl)-4,6-dichlorophenol (1.24 g, 4.8 mmol) in THF (20 mL) was added dropwise to a solution of 2-aminothiophenol (0.60 g, 4.8 mmol) and triethylamine (0.70 mL) in THF (20 mL) and stirred at room temperature for 12 h. The solid that had formed was filtered out, and the solvent was removed under vacuum. The crude product was dissolved in dichloromethane, washed with saturated NaCl solution, dried over $MgSO_4$, which was filtered out, and the solvent was removed under vacuum. The product was obtained as yellow oil in quantitative yield. ^{1}H NMR (400 MHz, $CDCl_3$), δ 7.21−7.09 (m, 3H, ArH), 6.78−6.59 (m, 3H, ArH), 4.44 (brs, 2H, $ArNH_2$), 3.90 (s, 2H, $ArCH_2S$).

Synthesis of Lig^1H_2. A solution of 2-((2-aminothiophenyl)methyl)-4,6-dichlorophenol (0.42 g, 1.4 mmol) in ethanol (20 mL) was added to a solution of 3,5-dichloro-2-hydroxybenzaldehyde (0.26 g, 1.4 mmol) in ethanol (20 mL) and stirred for 2 h at room temperature. The solvent was removed under vacuum yielding an orange solid in a final yield of 99%. ^{1}H NMR (500 MHz, $CDCl_3$), δ 8.41 (s, 1H, NCH), 7.44 (m, 2H, ArH), 7.33−7.27 (m, 3H, ArH), 7.18 (d, 1H, J = 10.7 Hz, ArH), 7.12 (d, 1H, J = 2.4 Hz, ArH), 6.87 (d, 1H, J = 2.4 Hz, ArH), 4.06 (s, 2H, $ArCH_2S$); ^{13}C NMR (125 MHz, $CDCl_3$), δ 159.0 (CN), 156.3 (C), 148.6 (C), 147.2 (C), 133.4 (CH), 131.8 (CH), 131.7 (C), 130.3 (CH), 129.0 (CH), 128.7 (CH), 127.7 (CH), 127.2(CH), 126.7 (C), 125.3 (C), 123.7 (C), 123.4 (C), 121.1 (C), 120.5 (C), 118.0 (CH), 33.5 (CH_2). MS(ESI): Calc for $C_{20}H_{13}Cl_4NO_2S$: 470.9, found: 469.9 (M-H$^+$). Anal. Calcd For $C_{20}H_{13}Cl_4NO_2S$: C, 50.76; H, 2.77; N, 2.96. Found: C, 50.52; H, 2.56; N, 2.83.

2-((2-Aminothiophenyl)methyl)-4,6-dibromophenol. was prepared from 2-(bromomethyl)-4,6-dibromophenol (1.48 g, 4.3 mmol) and 2-aminothiophenol according to the procedure described above for the dichloro-analogue and was obtained in quantitative yield. ^{1}H NMR (400 MHz, $CDCl_3$), δ 7.46 (d, 1H, J = 4.8 Hz, ArH), 7.20−7.09 (m, 2H, ArH), 6.92 (d, 1H, J = 4.8 Hz, ArH), 6.76−6.60 (m, 2H, ArH), 4.24 (brs, 2H, $ArNH_2$), 3.90 (s, 2H, $ArCH_2S$).

Synthesis of Lig^2H_2. A solution of 2-((2-aminothiophenyl)methyl)-4,6-dibromophenol (1.35 g, 3.5 mmol) in ethanol (20 mL) was added to a solution of 3,5-dibromo-2-hydroxybenzaldehyde (0.97 g, 3.5 mmol) in ethanol (20 mL) and stirred for 7 h at room temperature. The solvent was removed under vacuum and the crude product was purified by flash chromatography over Silica gel 60 with a mixture of petroleum ether: dichloromethane in increasing polarity as eluent. The pure product was obtained as red solid in a final yield of 35%. ^{1}H NMR (500 MHz, $CDCl_3$), δ 8.35 (s, 1H, NCH), 7.73 (d, 1H, J = 1.7 Hz, ArH), 7.46−7.43 (m, 2H, ArH), 7.36−7.32 (m, 2H, ArH), 7.27 (d, 1H, J = 10.1 Hz, ArH), 7.16 (d, 1H, J = 13.8 Hz, ArH), 6.96 (d, 1H, J = 1.3 Hz, ArH), 4.03 (s, 2H, $ArCH_2S$); ^{13}C NMR (125 MHz, $CDCl_3$), δ 159.8 (CN), 157.6 (C), 149.8 (C), 147.3 (C), 138.6 (CH), 133.7 (CH), 133.2 (CH), 132.5 (CH), 132.4 (CH), 131.5 (C), 128.8 (CH), 128.7(CH), 127.1 (C), 121.1 (C), 118.1 (CH), 112.8 (C), 112.5 (C), 111.5 (C), 110.5 (C), 34.0 (CH_2). MS(ESI): Calc for $C_{20}H_{13}Br_4NO_2S$: 646.7, found: 645.7 (M-H$^+$). Anal. Calcd For $C_{20}H_{13}Br_4NO_2S$: C, 36.90; H, 2.01; N, 2.15. Found: C, 37.6; H, 1.71; N, 2.10.

Synthesis of Lig^3H_2. A solution of 2-((2-aminothiophenyl)methyl)-4,6-dichlorophenol (1.03 g, 3.4 mmol) in ethanol (20 mL) was added to a solution of 3,5-dibromo-2-hydroxybenzaldehyde (0.96 g, 3.4 mmol) in ethanol (20 mL) and stirred for 12 h at room temperature. Lig^3H_2 was isolated as described for Lig^2H_2 as an orange solid in a final yield of 30%. ^{1}H NMR (500 MHz, $CDCl_3$), δ 8.37 (s, 1H, NCH), 7.74 (d, 1H, J = 2.0 Hz, ArH), 7.45−7.43 (m, 2H, ArH), 7.33−7.25 (m, 2H, ArH), 7.16 (d, 1H, J = 7.5 Hz, ArH), 7.11 (d, 1H, J = 2.0 Hz, ArH), 6.86 (d, 1H, J = 2.0 Hz, ArH), 4.05 (s, 2H, $ArCH_2S$); ^{13}C NMR (125 MHz, $CDCl_3$), δ 159.9 (CN), 157.6 (C), 148.5 (C), 147.2 (C), 138.6 (CH), 133.7 (CH), 132.0 (CH), 131.6 (C), 129.0 (CH), 128.7 (CH), 128.6 (CH), 127.7 (CH), 126.7(C), 125.3 (C), 121.1 (C), 121.0 (C), 118.1 (CH), 112.7 (C), 110.5 (C), 33.5 (CH_2). MS(ESI): Calc for $C_{20}H_{13}Br_2Cl_2NO_2S$: 558.8, found: 557.8 (M-H$^+$). Anal. Calcd For $C_{20}H_{13}Br_2Cl_2NO_2S$: C, 42.73; H, 2.33; N, 2.49. Found: C, 42.11; H, 2.17; N, 2.51.

Synthesis of Lig^4H_2. A solution of 2-((2-aminothiophenyl)methyl)-4,6-dibromophenol (1.23 g, 3.2 mmol) in ethanol (20 mL) was added to a solution of 3,5-dichloro-2-hydroxybenzaldehyde (0.60 g, 3.2 mmol) in ethanol (20 mL) and stirred for 12 h at room temperature. Lig^4H_2 was isolated as described for Lig^2H_2 as an orange-red solid in a final yield of 30%. ^{1}H NMR (500 MHz, $CDCl_3$), δ 8.38 (s, 1H, NCH), 7.44 (m, 2H, ArH), 7.36 (d, 1H, J = 1.9 Hz, ArH), 7.35−7.32 (m, 1H, ArH), 7.28 (d, 1H, J = 7.3 Hz, ArH), 7.26 (m, 1H, ArH), 7.17 (d, 1H, J = 7.6 Hz, ArH), 6.97(d, 1H, J = 1.7 Hz, ArH) 4.03 (s, 2H, $ArCH_2S$); ^{13}C NMR (125 MHz, $CDCl_3$), δ 159.9 (CN), 156.2 (C), 149.8 (C), 147.3 (C), 133.3 (CH), 133.2 (CH), 132.5 (CH), 132.3 (CH), 131.6 (C), 129.9 (CH), 128.8 (CH), 128.7 (CH), 127.0(C), 123.6 (C), 123.4 (C), 120.5 (C), 118.0 (CH), 112.4 (C), 111.5 (C), 33.9 (CH_2). MS(ESI): Calc for $C_{20}H_{13}Cl_2Br_2NO_2S$: 558.8, found: 557.8 (M-H$^+$). Anal. Calcd For $C_{20}H_{13}Cl_2Br_2NO_2S$: C, 42.73; H, 2.33; N, 2.49. Found: C, 42.05; H, 2.13; N, 2.11.

Synthesis of Lig^5H_2. A solution of 2-((2-aminothiophenyl)methyl)-4,6-dichlorophenol (0.60 g, 2.0 mmol) in benzene (20 mL) was added to a solution of 3,5-di-*tert*-butyl-2-hydroxybenzaldehyde (0.15 g, 2.0 mmol) in benzene (20 mL) and refluxed for 5 h. The solvent was removed under vacuum and the crude product was purified by flash chromatography on Silica gel 60 with a mixture of petroleum ether: dichloromethane in increasing polarity as eluent. The pure product was obtained as an orange solid in a final yield of 71%. ^{1}H NMR (500 MHz, $CDCl_3$), δ 8.49 (s, 1H, NCH), 7.46 (s, 1H, ArH), 7.39 (d, 1H, J = 7.6 Hz, ArH), 7.30 (m, 1H, ArH), 7.19 (m, 2H, ArH), 7.14−7.12 (m, 1H, ArH), 6.94 (s, 1H, ArH), 4.06 (s, 2H, $ArCH_2S$), 1.49 (s, 9H, $C(CH_3)_3$), 1.33 (s, 9H, $C(CH_3)_3$); ^{13}C NMR (125 MHz, $CDCl_3$), δ 164.0 (CN), 158.6 (C), 149.4 (C), 148.5 (C), 140.8 (C), 137.4 (C), 132.1 (C), 131.7 (CH), 130.4 (C), 129.1 (CH), 128.6 (CH), 128.5 (CH), 128.1 (C), 127.7 (CH), 127.3 (CH), 127.2 (CH), 126.8 (C), 125.2 (C), 118.6 (CH), 33.3 (CH_2), 31.7 (CH_3), 31.5(C), 29.7(CH_3), 29.5 (C).). MS(ESI): Calc for $C_{28}H_{31}Cl_2NO_2S$: 515.1, found: 516.0 (MH$^+$). Anal. Calcd For $C_{28}H_{31}Cl_2NO_2S$: C, 65.11; H, 6.05; N, 2.71. Found: C, 64.88; H, 5.89; N, 2.70.

2-((2-Aminothiophenyl)methyl)-4,6-di-tert-butylphenol. was prepared from 2-(bromomethyl)-4,6-di-*tert*-butylphenol (1.03 g, 3.4 mmol) and 2-aminothiophenol (0.43 g, 3.4 mmol) according to the procedure described above for the dichloro-analogue and was obtained as yellow oil in quantitative yield. ^{1}H NMR (400 MHz, $CDCl_3$), δ 7.24 (d, 1H, J = 2.0 Hz, ArH), 7.13−7.03 (m, 2H, ArH), 6.74−6.52 (m, 3H, ArH), 4.31 (brs, 2H, $ArNH_2$), 3.95 (s, 2H, $ArCH_2S$), 1.37 (s, 9H, $C(CH_3)_3$), 1.16 (s, 9H, $C(CH_3)_3$).

Synthesis of Lig^6H_2. A solution of 2-((2-aminothiophenyl)methyl)-4,6-di-*tert*-butylphenol (1.00 g, 2.9 mmol) in ethanol (20 mL) was added to a solution of 3,5-dichloro-2-hydroxybenzaldehyde (0.55 g, 2.9 mmol) in ethanol (20 mL) and stirred for 2 h at room temperature. Lig^6H_2 was isolated as described for Lig^2H_2 as an orange-red solid in a final yield of 69%. ^{1}H NMR (500 MHz, $CDCl_3$), δ 8.50 (s, 1H, NCH), 7.47 (s, 1H, ArH), 7.42 (d, 1H, J = 7.6 Hz, ArH), 7.31−7.28 (m, 2H, ArH), 7.25−7.21 (m, 2H, ArH), 7.18−7.16 (m, 2H, ArH), 4.12 (s, 2H, $ArCH_2S$), 1.37 (s, 9H, $C(CH_3)_3$), 1.20 (s, 9H, $C(CH_3)_3$); ^{13}C NMR (125 MHz, $CDCl_3$), δ 160.5 (CN), 156.4 (C), 151.5 (C), 147.3 (C), 142.7 (C), 137.3 (CH), 133.3 (CH), 132.3 (CH), 130.8 (C), 130.3 (C), 130.1 (CH), 128.7 (CH), 128.4(CH), 125.5 (CH), 124.1 (CH), 123.6 (C), 121.8 (C), 120.5 (C), 118.1 (CH), 36.5 (CH_2), 35.1 (C), 34.4 (C), 31.7 (CH_3), 30.0 (CH_3). MS(ESI): Calc for $C_{28}H_{31}Cl_2NO_2S$: 515.1, found: 514.1 (M-H$^+$). Anal. Calcd For $C_{28}H_{31}Cl_2NO_2S\bullet C_2H_6O$: C, 64.38; H, 6.26; N, 2.36. Found: C, 64.05; H, 6.62 ; N, 2.49.

Synthesis of Lig^7H_2. A solution of 2-((2-aminothiophenyl)methyl)-4,6-dichlorophenol (0.82 g, 2.7 mmol) in benzene (20 mL) was added to a solution of 3-adamantyl-2-hydroxy-5-methylbenzaldehyde (0.74 g,

dx.doi.org/10.1021/ic501164c | Inorg. Chem. 2014, 53, 9140−9150

2.7 mmol) in benzene (20 mL) and refluxed for 5 h. Lig^7H_2 was isolated as described for Lig^2H_2 as an orange-red solid in a final yield of 50%. ^{1}H NMR (500 MHz, $CDCl_3$), δ 8.47 (s, 1H, NCH), 7.41 (dd, 1H, J = 7.7, 1.4 Hz, ArH), 7.33−7.30 (m, 1H, ArH), 7.23−7.21 (m, 1H, ArH), 7.18 (d, 2H, J = 2.44 Hz, ArH), 7.13 (dd, 1H, J = 7.7, 1.4 Hz, ArH),7.04 (s, 1H, ArH), 6.99 (d, 1H, J = 2.44 Hz, ArH), 4.09 (s, 2H, $ArCH_2S$), 2.33 (s, 3H, $ArCH_3$) 2.24 (m, 5H, Ad), 2.13 (m, 3H, Ad), 1.81 (m, 7H, Ad); ^{13}C NMR (125 MHz, $CDCl_3$), δ 163.9 (CN), 159.0 (C), 156.5 (C), 133.3 (C), 132.5 (C), 132.2 (C), 131.7 (C), 130.8 (CH), 130.0 (C), 129.1 (C), 128.9 (C), 128.8 (C), 128.6(CH), 128.5 (CH), 127.7 (CH), 127.2 (CH), 118.6 (CH), 118.2 (CH), 40.9 (CH_2), 40.5 (CH_2), 37.4 (CH_3), 37.3 (CH_2), 33.3 (C), 29.3 (CH_2). MS(ESI): Calc for $C_{31}H_{31}Cl_2NO_2S$: 551.15, found: 550.1 (M-H$^+$). Anal. Calcd For $C_{31}H_{31}Cl_2NO_2S{\cdot}C_6H_6$: C, 70.46; H, 5.91; N, 2.22. Found: C, 69.84; H, 6.06; N, 2.37.

2-((2-Aminothiophenyl)methyl)-4-methyl-6-adamantylphenol. was prepared from 2-(bromomethyl)-4-methyl-6-adamanthylphenol (1.00 g, 3.0 mmol) and 2-aminothiophenol (0.37 g, 3.0 mmol) according to the procedure described above for the dichloro-analogue and was obtained as yellow oil in quantitative yield. ^{1}H NMR (400 MHz, $CDCl_3$), δ 7.21−7.08 (m, 2H, ArH), 6.89 (d, 1H, J = 2.0 Hz, ArH), 6.73−6.69 (m, 1H, ArH), 6.65 (d, 1H, J = 2.0 Hz, ArH), 6.63−6.58 (m, 1H, ArH), 4.33 (brs, 2H, $ArNH_2$), 3.94 (s, 2H, $ArCH_2S$), 2.17 (s, 3H, $ArCH_3$), 2.10(m, 3H, Ad), 2.06 (m, 6H, Ad), 1.77 (m, 6H, Ad).

Synthesis of Lig^8H_2. A solution of 2-((2-aminothiophenyl)methyl)-4-methyl-6-adamantylphenol (1.00 g, 2.6 mmol) in ethanol (20 mL) was added to a solution of 3,5-dichloro-2-hydroxybenzaldehyde (0.50 g, 2.6 mmol) in ethanol (20 mL) and stirred for 2 h at room temperature. Lig^8H_2 was isolated as described for Lig^2H_2 as an orange solid in a final yield of 55%. ^{1}H NMR (500 MHz, $CDCl_3$), δ 8.45 (s, 1H, NCH), 7.50−7.47 (m, 2H, ArH), 7.33−7.25 (m, 2H, ArH), 7.17 (d, 1H, J = 7.7 Hz, ArH), 6.89 (s, 1H, ArH), 6.63 (s, 1H, ArH), 5.86 (s, 1H, ArH), 4.07 (s, 2H, $ArCH_2S$), 2.15 (s, 3H, $ArCH_3$), 2.05(m, 9H, Ad), 1.75 (m, 6H, Ad); ^{13}C NMR (125 MHz, $CDCl_3$), δ 161.1 (CN), 156.5 (C), 151.9 (C), 147.4 (C), 138.2 (C), 133.3 (CH), 132.5 (CH), 130.8 (C), 130.0 (CH), 129.6 (C), 128.9 (CH), 128.8 (CH), 128.5(CH), 127.7 (CH), 123.6 (C), 122.7 (C), 120.4 (C), 118.2 (CH), 118.1 (C), 40.9 (CH_2), 37.3 (CH_2), 37.1 (C), 36.4 (CH_3), 29.3 (CH), 20.9 (CH_2) MS(ESI): Calc for $C_{31}H_{31}Cl_2NO_2S$: 551.1, found: 550.1 (M-H$^+$). Anal. Calcd For $C_{28}H_{13}Cl_2NO_2S{\bullet}C_2H_6O$: C, 66.21; H, 6.23; N, 2.34. Found: C, 65.99; H, 5.61; N, 2.21.

Synthesis of $Lig^1Zr(O\text{-}tert\text{-}Bu)_2$. Lig^1H_2 (26 mg, 0.05 mmol) was dissolved in 2 mL of ether and was added dropwise to a solution of $Zr(O^tBu)_4$ (21 mg, 0.05 mmol) in 2 mL of ether at RT. The solution was stirred for 2h after which the solid that has precipitated ($(Lig^1)_2Zr$) was filtered off, and the ether was removed under vacuum. Extraction with pentane and removal of the slowly precipitating $(Lig^1)_2Zr$ (twice) followed by crystallization at −35 °C gave $Lig^1Zr(O\text{-}tert\text{-}Bu)_2$ (23 mg) which still contained traces of $(Lig^1)_2Zr$. X-ray quality crystals of $Lig^1Zr(O\text{-}tert\text{-}Bu)_2$ were grown from ether at −35 °C. ^{1}H NMR (400 MHz, C_6D_6), δ 7.40 (d, 1H, J = 2.6 Hz, ArH), 7.13 (s, 1H, NCH), 7.00 (d, 1H, J = 4.4 Hz, ArH), 6.65 (d, J = 2.6, 1H, ArH), 6.62−6.51 (m, 4H, ArH), 4.36 (bs, 1H, CH_2), 3.35 (bs, 1H, CH_2), 1.37 (bs, 9H, $C(CH_3)_3$), 1.27 (bs, 9H, $C(CH_3)_3$); δ ^{13}C NMR (100.66 MHz, C_6D_6), δ 164.6 (CN), 158.6 (C), 158.0 (C), 152.6 (C), 135.9 (CH), 135.3 (CH), 134.7 (C), 133.5 (CH), 132.6 (C), 131.4 (CH), 128.9 (CH), 128.6 (CH), 128.5 (CH), 125.1 (C), 123.9 (C), 123.5 (C), 122.0 (CH), 120.9 (C), 120.6 (C), 39.3 (CH_2), 32.6 ($6CH_3$).

Crystal Data for Complex $[Lig^1Zr(O^tBu)_2]$. $C_{28}H_{29}Cl_4NO_4SZr$; M = 708.60; monoclinic; space group $P2_1/n$; a = 15.3814(5) Å, b = 10.3957(3) Å, c = 19.0391(7)Å, β = 92.1714(16)°, V = 3042.17(17) Å^3; T = 110(2) K; Z = 4; D_c = 1.547 g cm^{-3}; μ (Mo Kα) = 0.816 mm^{-1}; R_1 = 0.0465 and wR_2 = 0.0925 for 3563 reflections with $I > 2\sigma$ (I); R_1 = 0.0889 and wR_2 = 0.1090 for all 5368 unique reflections.

Synthesis of $(Lig^1)_2Zr$. Lig^1H_2 (46 mg, 0.10 mmol) was dissolved in 2 mL of ether and was added dropwise to a solution of $Zr(O^tBu)_4$ (19 mg, 0.05 mmol) in 2 mL of ether at RT. The solution was stirred for 2h during which a yellow solid precipitated. The solvent was removed under vacuum giving $(Lig^1)_2Zr$ in quantitative yield. ^{1}H NMR (400 MHz, C_6D_6), δ 7.44 (s, 2H, NCH), 7.37 (m, 2H, ArH), 7.26 (d, 2H, J = 2.5 Hz, ArH), 7.04 (d, 2H, J = 2.5 Hz, ArH), 6.88 (m, 4H, ArH), 6.65 (m, 2H, ArH), 6.33 (m, 4H, ArH), 3.88 (d, 2H, J = 13.8 Hz, CH_2), 3.36 (d, J = 13.8, 2H, CH_2); δ ^{13}C NMR (100.66 MHz, C_6D_6), 166.4 (CN), 159.7 (C), 157.0 (C), 156.6 (C), 137.6 (C), 135.4 (CH), 134.9 (CH), 131.7 (CH), 130.5 (CH), 129.5 (CH), 129.2 (CH), 127.1 (CH), 126.8 (C), 126.5 (C), 125.4 (C), 125.0 (C), 124.5 (C), 123.7 (C), 119.4 (CH), 38.9 (CH_2). Anal. Calcd for $C_{40}H_{22}Cl_8N_2O_4S_2Zr$: C, 46.48; H, 2.15; N, 2.71. Found: C, 46.08; H, 2.37; N, 2.01.

Synthesis of $Lig^2Zr(O\text{-}tert\text{-}Bu)_2$. Lig^2H_2 (52 mg, 0.08 mmol) was dissolved in 2 mL of ether and was added dropwise to a solution of $Zr(O^tBu)_4$ (31 mg, 0.08 mmol) in 2 mL of ether RT. The solution was stirred for 2h after which the solid that has precipitated ($(Lig^2)_2Zr$) was filtered off, and the ether was removed under vacuum to give 48 mg of almost pure $Lig^2Zr(O\text{-}tert\text{-}Bu)_2$. Extraction with pentane followed by crystallization at RT gave $Lig^2Zr(O\text{-}tert\text{-}Bu)_2$ (12 mg, 17%) as a red solid. X-ray quality crystals of $Lig^2Zr(O\text{-}tert\text{-}Bu)_2$ were grown from ether at −35 °C. ^{1}H NMR (400 MHz, C_6D_6), δ 7.88 (d, 1H, J = 8.0 Hz, ArH), 7.74 (d, 1H, J = 2.1 Hz, ArH), 7.31 (d, 1H, J = 2.1 Hz, ArH), 7.05 (s, 1H, NCH), 6.64 (m, 2H, ArH), 6.53 (m, 2H, ArH), 6.37 (d, 1H, J = 8.0 Hz, ArH), 4.42 (bs, 1H, CH_2), 3.35 (bs, 1H, CH_2), 1.43 (bs, 9H, $C(CH_3)_3$), 1.30 (bs, 9H, $C(CH_3)_3$); ^{13}C NMR (100.66 MHz, C_6D_6), δ 166.5 (CN), 159.2 (C), 156.2 (C), 152.6 (CH), 152.0 (C), 135.7 (CH), 140.8 (CH), 135.7 (CH), 135.0 (CH), 132.3 (CH), 130.4 (CH), 127.0 (CH), 124.3 (C), 124.1 (C), 123.4 (C), 117.2 (C), 114.9 (C), 108.0 (C), 107.7 (C), 65.9 (CH_2), 39.0 (C), 34.2 (C), 33.0 ($6CH_3$). Anal. Calcd for $C_{28}H_{29}Br_4NO_4SZr$: C, 37.94; H, 3.30; N, 1.58. Found: C, 35.23; H, 3.16; N, 1.25.

Crystal Data for Complex $[Lig^2Zr(O^tBu)_2]$. $C_{28}H_{29}Br_4NO_4SZr$; M = 886.44; monoclinic; space group $P2_1/n$; a = 15.5039(2) Å, b = 10.5403(10) Å, c = 19.2366(3)Å, β = 91.8978(6)°, V = 3141.84(7) Å^3; T = 110(2) K; Z = 4; D_c = 1.874 g cm^{-3}; μ (Mo Kα) = 5.537 mm^{-1}; R_1 = 0.0310 and wR_2 = 0.0665 for 7444 reflections with $I > 2\sigma$ (I); R_1 = 0.0484 and wR_2 = 0.0665 for all 5368 unique reflections.

Synthesis of $(Lig^2)_2Zr$. $(Lig^2)_2Zr$ was prepared in quantitative yield from Lig^2H_2 (53 mg, 0.095 mmol) and $Zr(O^tBu)_4$ (18 mg, 0.047 mmol) as described above for $(Lig^1)_2Zr$. ^{1}H NMR (400 MHz, C_6D_6), δ 7.54 (s, 2H, ArH), 7.46 (s, 2H, NCH), 7.35 (s, 2H, ArH), 7.25 (m, 2H, ArH), 6.81 (d, J = 2.0, 4H, ArH), 6.76 (s, 2H, ArH) 6.48 (m, 2H, ArH), 6.37 (m, 2H, ArH), 3.92 (d, 2H, J = 13.7 Hz, CH_2), 3.34 (d, J = 13.7, 2H, CH_2); ^{13}C NMR (100.66 MHz, C_6D_6), δ 164.5 (CN), 159.2 (C), 159.0 (C), 156.2 (C), 140.7 (CH), 137.6 (CH), 135.4 (CH), 134.6 (CH), 132.4 (CH), 131.1 (CH), 129.3 (C), 128.5 (CH), 125.6 (C), 125.5 (C), 125.1 (C), 121.9 (CH), 115.6 (C), 114.6 (C), 109.0 (C), 65.9 (CH_2). Anal. Calcd for $C_{40}H_{22}Br_8N_2O_4S_2Zr$: C, 34.58; H, 1.60; N, 2.02. Found: C, 33.26; H, 1.59; N, 1.63.

Synthesis of $Lig^3Zr(O\text{-}tert\text{-}Bu)_2$. Lig^3H_2 (31 mg, 0.05 mmol) was dissolved in 2 mL of ether and was added dropwise to a solution of $Zr(O^tBu)_4$ (21 mg, 0.05 mmol) in 2 mL of ether at RT. The solution was stirred for 2h after which the solid that has precipitated ($(Lig^3)_2Zr$) was filtered off, and the ether was removed under vacuum. Extraction with pentane followed by crystallization at RT gave $Lig^3Zr(O\text{-}tert\text{-}Bu)_2$ (16 mg, 37%) as a red solid. ^{1}H NMR (400 MHz, C_6D_6), δ 7.83 (d, 1H, J = 2.0 Hz, ArH), 7.18 (s, 1H, NCH), 7.10 (d, 1H, J = 2.0 Hz, ArH), 6.73 (m, 2H, ArH), 6.68−6.61 (m, 2H, ArH), 6.56 (d, 1H, J = 2.0 Hz, ArH), 6.44 (m, 1H, ArH), 4.53 (bs, 1H, CH_2), 3.43 (bs, 1H, CH_2), 1.48 (bs, 9H, $C(CH_3)_3$), 1.13 (bs, 9H, $C(CH_3)_3$); ^{13}C NMR (100.66 MHz, C_6D_6), δ 166.5 (CN), 160.7 (C), 157.0 (C), 152.5 (C), 140.9 (CH), 135.7 (CH), 135.0 (CH), 130.4 (CH), 129.5 (CH), 129.3 (CH), 127.0 (CH), 124.5 (C), 124.3 (C), 123.7 (C), 123.5 (C), 120.6 (C), 117.2 (C), 108.0 (C), 39.5 (CH_2), 32.6 (CH_3), 31.3 (CH_3). Anal. Calcd for $C_{28}H_{29}Cl_2Br_2NO_4SZr$: C, 42.17; H, 3.67; N, 1.76. Found: C, 40.00; H, 2.99; N, 1.39.

Synthesis of $(Lig^3)_2Zr$. $(Lig^3)_2Zr$ was prepared in quantitative yield from Lig^3H_2 (55 mg, 0.10 mmol) and $Zr(O^tBu)_4$ (19 mg, 0.05 mmol) as described above for $(Lig^1)_2Zr$. ^{1}H NMR (400 MHz, C_6D_6), δ 7.66 (d, 2H, J = 1.9 Hz, ArH), 7.54 (s, 2H, NCH), 7.38 (m, 2H, ArH), 7.12 (d, 2H, J = 1.9 Hz, ArH), 6.91 (m, 4H, ArH), 6.88 (d, 2H, J = 2.0 Hz,

dx.doi.org/10.1021/ic501164c | Inorg. Chem. 2014, 53, 9140−9150

ArH) 6.44 (m, 2H, ArH), 6.41 (d, 2H, J = 2.0 Hz, ArH), 3.99 (d, 2H, *J* = 13.8 Hz, CH_2), 3.44 (d, *J* = 13.8, 2H, CH_2); ^{13}C NMR (100.66 MHz, C_6D_6), δ 164.7 (CN), 159.1 (C), 158.1 (C), 156.5 (C), 140.8 (CH), 137.4 (CH), 135.6 (CH), 131.2 (CH), 129.2 (CH), 128.9 (CH), 128.8 (CH), 128.5 (CH), 125.6 (C), 125.5 (C), 124.9 (C), 124.1 (C), 122.0 (CH), 121.4 (C), 115.6 (C), 109.0 (C), 65.9 (CH_2). Anal. Calcd for $C_{40}H_{22}Cl_4Br_4N_2O_4S_2Zr$: C, 39.66; H, 1.83; N, 2.31. Found: C, 36.49; H, 1.63; N, 1.85.

Synthesis of Lig^{4}Zr(O-tert-Bu)$_2$. Lig^{4}H$_2$ (33 mg, 0.06 mmol) was dissolved in 2 mL of ether and was added dropwise to a solution of Zr(O^{t}Bu)$_4$ (23 mg, 0.06 mmol) in 2 mL of ether at RT. The solution was stirred for 2 h after which the solid that has precipitated ((Lig^4)$_2$Zr) was filtered off, and the ether was removed under vacuum. Extraction with pentane followed by crystallization at RT gave Lig^{4}Zr(O-*tert*-Bu)$_2$ (11 mg, 22%) as a red solid. X-ray quality crystals of Lig^{4}Zr(O-*tert*-Bu)$_2$ were grown from ether at −35 °C. ^1H NMR (400 MHz, C_6D_6), δ 7.48 (d, 1H, *J* = 2.3 Hz, ArH), 7.45 (d, 1H, *J* = 1.7 Hz, ArH), 7.22 (s, 1H, NCH), 6.74 (d, 1H, *J* = 2.3 Hz, ArH), 6.72 (d, 1H, J = 1.7 Hz, ArH), 6.64 (m, 2H, ArH), 6.46 (m, 2H, ArH), 4.51 (bs, 1H, CH_2), 3.46 (bs, 1H, CH_2), 1.40 (bs, 9H, $C(CH_3)_3$), 1.14 (bs, 9H, $C(CH_3)_3$); ^{13}C NMR (100.66 MHz, C_6D_6), δ 166.4 (CN), 159.8 (C), 156.4 (C), 152.6 (C), 135.7 (CH), 135.0 (CH), 134.6 (CH), 133.7 (CH), 131.8 (CH), 130.5 (CH), 128.5 (CH), 127.5 (C), 127.0 (CH), 125.5 (C), 125.1 (C), 124.1 (C), 121.2 (C), 114.6 (C), 108.7 (C), 39.4 (C), 39.0 (C), 32.6 (CH_3), 31.4 (CH_3). Anal. Calcd for $C_{28}H_{29}Br_2Cl_2NO_4SZr$: C, 42.17; H, 3.67; N, 1.76. Found: C, 41.75; H, 3.39; N, 1.40.

Crystal Data for Complex [Lig^{4}Zr(O^{t}Bu)$_2$]. $C_{28}H_{29}Br_2Cl_2NO_4SZr$; M = 797.52; monoclinic; space group $P2_1/n$; *a* = 15.4730(3) Å, *b* = 10.3699(2) Å, *c* = 19.0831(4) Å, β = 91.3090(10)°, *V* = 3059.46(11) Å^3; *T* = 110(2) K; *Z* = 4; D_c = 1.731 g cm^{-3}; μ (Mo Kα) = 3.249 mm^{-1}; R_1 = 0.0261 and wR_2 = 0.0624 for 6810 reflections with $I > 2\sigma$ (I); R_1 = 0.0312 and wR_2 = 0.0644 for all 7633 unique reflections.

Synthesis of (Lig^4)$_2$Zr. (Lig^4)$_2$Zr was prepared in quantitative yield from Lig^{4}H$_2$ (44 mg, 0.068 mmol) and Zr(O^{t}Bu)$_4$ (13 mg, 0.034 mmol) as described above for (Lig^1)$_2$Zr. ^1H NMR (400 MHz, C_6D_6), δ 7.45 (s, 2H, NCH), 7.38 (d, 2H, *J* = 1.7 Hz, ArH), 7.35 (d, 2H, *J* = 6.9 Hz, ArH), 7.24 (d, 2H, *J* = 2.2 Hz, ArH), 6.85 (m, 4H, ArH), 6.60 (d, 2H, *J* = 2.0 Hz, ArH) 6.50 (d, 2H, *J* = 2.0 Hz, ArH), 6.34 (d, 2H, *J* = 7.4 Hz, ArH), 3.89 (d, 2H, *J* = 13.8 Hz, CH_2), 3.35 (d, *J* = 13.8, 2H, CH_2); ^{13}C NMR (100.66 MHz, C_6D_6), δ 164.4 (CN), 159.6 (C), 158.3 (C), 158.0 (C), 135.4 (CH), 135.2 (CH), 134.9 (CH), 132.8 (CH), 132.2 (CH), 131.3 (CH), 126.8 (C), 125.4 (C), 123.9 (C), 123.4 (C), 122.1 (C), 121.9 (CH), 119.3 (CH), 114.9 (C), 107.7 (C), 65.9 (CH_2). Anal. Calcd for $C_{40}H_{22}Br_4Cl_4N_2O_4S_2Zr$: C, 39.66; H, 1.83; N, 2.31. Found: C, 38.04; H, 1.68; N, 1.88.

Synthesis of Lig^{5}Zr(O-tert-Bu)$_2$. Lig^{5}H$_2$ (44 mg, 0.09 mmol) was dissolved in 2 mL of ether and was added dropwise to a solution of Zr(O^{t}Bu)$_4$ (33 mg, 0.09 mmol) in 2 mL of ether at RT. The solution was stirred for 2h after which the solvent was removed under vacuum resulting in a yellow solid in quantitative yield (64 mg). ^1H NMR (400 MHz, C_6D_6), δ 7.79 (s, 1H, NCH), 7.75 (s, 1H, ArH), 7.09 (s, 1H, ArH), 7.02 (m, 2H, ArH), 6.73 (t, 1H, *J* = 7.5 Hz, ArH), 6.68 (t, 1H, *J* = 7.2 Hz, ArH), 6.35 (m, 2H, ArH), 3.91 (d, 1H, *J* = 12.4, CH_2), 3.27 (d, 1H, *J* = 12.4, CH_2), 1.77 (s, 9H, $C(CH_3)_3$), 1.51 (bs, 9H, $C(CH_3)_3$), 1.34 (s, 9H, $C(CH_3)_3$), 1.12 (bs, 9H, $C(CH_3)_3$); ^{13}C NMR (100.66 MHz, C_6D_6), δ 167.3 (CN), 162.2 (C), 159.1 (C), 154.1 (C), 140.2 (C), 139.4 (C), 136.0 (CH), 132.0 (CH), 131.6 (CH), 130.7 (CH), 129.7 (CH), 127.1 (CH), 124.7 (C), 123.8 (C), 123.7 (C), 123.3 (C), 120.0 (CH), 119.4 (C), 40.4 (CH_2), 33.3 (CH_3), 32.5 (CH_3), 31.6 (CH_3), 31.5 (C), 31.1 (C), 30.0 (CH_3). Anal. Calcd for $C_{36}H_{47}Cl_2NO_4SZr$: C, 57.50; H, 6.30; N, 1.86. Found: C, 57.90; H, 6.61; N, 1.52.

Synthesis of Lig^{6}Zr(O-tert-Bu)$_2$. Lig^{6}Zr(O-*tert*-Bu)$_2$ was synthesized as a yellow solid in quantitative yield (53 mg) as described above for Lig^{5}Zr(O-*tert*-Bu)$_2$ from Lig^{6}H$_2$ (37 mg, 0.07 mmol) and Zr(O^{t}Bu)$_4$ (28 mg, 0.07 mmol). X-ray quality crystals of Lig^{6}Zr(O-*tert*-Bu)$_2$ were grown from ether at −35 °C. ^1H NMR (400 MHz, C_6D_6), δ 7.43 (d, 1H, *J* = 2.2 Hz, ArH), 7.13 (s, 1H, NCH), 6.76 (s, 1H, ArH), 6.66 (d, 1H, J = 2.2 Hz, ArH), 6.59 (t, 2H, *J* = 6.1 Hz, ArH), 6.47 (m, 2H, ArH), 6.40 (m, 2H, ArH), 5.04 (d, 1H, *J* = 11.9, CH_2), 3.78 (d, 1H, *J* = 11.9, CH_2), 1.60 (s, 9H, $C(CH_3)_3$), 1.35 (s, 9H, $C(CH_3)_3$), 1.34 (s, 9H, $C(CH_3)_3$), 1.21 (bs, 9H, $C(CH_3)_3$); ^{13}C NMR (100.66 MHz, C_6D_6), δ 167.2 (CN), 160.3 (C), 158.2 (C), 152.2 (C), 139.2 (C), 136.8 (C), 135.2 (CH), 135.0 (CH), 131.3 (CH), 128.9 (CH), 127.1 (CH), 125.8 (CH), 124.4 (C), 123.6 (C), 123.4 (CH), 121.4 (C), 120.2 (C), 119.1 (CH), 77.7 (C), 77.4 (C), 39.7 (CH_2), 35.2 (C), 34.2 (C), 32.9 (CH_3), 32.7 (CH_3), 32.0 (CH_3), 29.9 (CH_3). Anal. Calcd for $C_{32}H_{47}Cl_2NO_4SZr{\cdot}H_2O$: C, 56.16; H, 6.41; N, 1.82. Found: C, 56.09; H, 6.21; N, 1.75.

Crystal Data for Complex [Lig^{6}Zr(O^{t}Bu)$_2$]. $C_{36}H_{47}Cl_2NO_4SZr{\cdot}C_4H_{10}O$; M = 826.05; triclinic; space group *P*-1; *a* = 12.7728(2) Å, *b* = 12.8029(2) Å, *c* = 14.5862(2) Å, α = 72.1301(6)°, β = 71.0202(6)°, γ = 86.4523(6)°, *V* = 2144.86(6) Å^3; *T* = 110(2) K; *Z* = 2; D_c = 1.279 g cm^{-3}; μ (Mo Kα) = 0.470 mm^{-1}; R_1 = 0.0446 and wR_2 = 0.1072 for 7750 reflections with $I > 2\sigma$ (I); R_1 = 0.0657 and wR_2 = 0.1188 for all 10012 unique reflections.

Synthesis of Lig^{7}Zr(O-tert-Bu)$_2$. Lig^{7}Zr(O-*tert*-Bu)$_2$ was synthesized as an orange solid in quantitative yield as described above for Lig^{5}Zr(O-*tert*-Bu)$_2$ from Lig^{7}H$_2$ (35 mg, 0.06 mmol) and Zr(O^{t}Bu)$_4$ (24 mg, 0.06 mmol). ^1H NMR (400 MHz, C_6D_6), δ 7.82 (s, 1H, NCH), 7.39 (s, 1H, ArH), 7.14 (s, 1H, ArH), 7.08 (s, 1H, ArH), 6.86 (t, 1H, *J* = 7.4 Hz, ArH), 6.80 (t, 1H, *J* = 6.9, ArH), 6.72 (s, 1H, ArH), 6.54 (d, 1H, *J* = 7.7, ArH), 3.91 (d, 1H, *J* = 12.9, CH_2), 3.33 (d, 1H, *J* = 12.9, CH_2), 2.57 (m, 7H, Ad), 2.31 (m, 5H, Ad), 2.11 (m, 3H, Ad), 1.96 (m, 4H, Ad), 1.62 (s, 9H, $C(CH_3)_3$), 1.18 (s, 9H, $C(CH_3)_3$); ^{13}C NMR (100.66 MHz, C_6D_6), δ 166.7 (CN), 162.4 (C), 161.1 (C), 159.5 (C), 154.1 (C), 139.9 (C), 136.1 (CH), 134.3 (CH), 131.8 (CH), 129.7 (CH), 127.4 (CH), 126.8 (C), 124.7 (C), 124.5 (C), 123.9 (C), 123.2 (C), 120.0 (CH), 75.6 (C), 72.7 (C), 40.9 (CH_2), 40.8 (Ad), 37.6 (CH_3), 33.1 (Ad), 32.4 (CH_3), 31.3 (Ad), 29.7 (Ad). Anal. Calcd for $C_{32}H_{47}Cl_2NO_4SZr{\cdot}C_7H_8$: C, 62.77; H, 6.30; N, 1.59. Found: C, 62.93; H, 6.79; N, 1.08.

Synthesis of Lig^{8}Zr(O-tert-Bu)$_2$. Lig^{8}Zr(O-*tert*-Bu)$_2$ was synthesized as an orange solid in quantitative yield (67 mg) as described above for Lig^{5}Zr(O-*tert*-Bu)$_2$ from Lig^{8}H$_2$ (41 mg, 0.07 mmol) and Zr(O^{t}Bu)$_4$ (29 mg, 0.07 mmol). ^1H NMR (400 MHz, C_6D_6), δ 7.56 (s, 1H, NCH), 7.39 (d, 1H, *J* = 2.4 Hz, ArH), 6.92 (s, 1H, ArH), 6.90 (d, 1H, *J* = 7.6 Hz, ArH), 6.78 (d, 1H, *J* = 2.4 Hz, ArH), 6.72−6.65 (m, 2H, ArH), 6.55 (d, 1H, *J* = 7.6 Hz, ArH), 6.37 (s, 1H, ArH), 4.68 (d, 1H, *J* = 12.4, CH_2), 3.81 (d, 1H, *J* = 12.4, CH_2), 2.22 (m, 5H, Ad), 2.16 (m, 3H, Ad), 2.06 (m, 3H, Ad), 2.00 (m, 4H, Ad), 1.84 (m, 4H, Ad), 1.34 (s, 9H, $C(CH_3)_3$), 1.15 (s, 9H, $C(CH_3)_3$); ^{13}C NMR (100.66 MHz, C_6D_6), δ 164.7 (CN), 158.9 (C), 152.1 (C), 137.7 (C), 135.8 (CH), 135.3 (CH), 132.7 (CH), 130.1 (CH), 129.8 (CH), 127.5 (CH), 126.8 (C), 126.5 (C), 124.8 (C), 124.4 (C), 124.2 (C), 121.2 (C), 120.1 (C), 119.7 (CH), 80.8 (C), 73.9 (C), 40.7 (CH_2), 37.4 (Ad), 37.0 (Ad), 32.9 (CH_3), 32.6 (Ad), 31.3 (CH_3), 29.8 (Ad). Anal. Calcd for $C_{39}H_{47}Cl_2NO_4SZr{\cdot}H_2O$: C, 58.12; H, 6.13; N, 1.74. Found: C, 57.69; H, 5.59; N, 1.67.

Synthesis of [{ONSO$^{(ethylene)}$}Hf(O-t-Bu)$_2$]. Ligand precursor {ONSO}^{ethylene}H$_2$[15] (48 mg, 0.09 mmol) was dissolved in ca. 2 mL of ether and was added dropwise to a solution of Hf(O^{t}Bu)$_4$ (44 mg, 0.09 mmol) at room temperature. The solution was stirred for 2h after which the solvent was removed under vacuum giving the target hafnium complex in quantitative yield (79 mg). ^1H NMR (500 MHz, C_6D_6), δ 7.72 (d, 1H, *J* = 2.3 Hz, ArH), 7.56 (s, 1H, ArH), 7.16 (s, 1H, ArH), 6.92 (s, 1H, NCH), 6.88 (d, *J* = 2.0, 1H, ArH), 4.28 (m, 1H, CH), 3.57 (d, 1H, *J* = 13.4 Hz, CH_2), 2.25 (m, 1H, CH), 1.87 (d, 1H, J = 11.7 Hz, CH_2), 1.77 (s, 9H, $C(CH_3)_3$), 1.57 (s, 9H, $C(CH_3)_3$), 1.47 (s, 9H, $C(CH_3)_3$), 1.37 (s, 18H, $C(CH_3)_3$), 1.30 (s, 9H, $C(CH_3)_3$); ^{13}C NMR (125 MHz, C_6D_6), δ 160.5 (CN), 139.3 (CH), 138.7 (C), 137.9 (C), 129.7 (CH), 128.1 (CH), 127.9 (C), 127.7 (C), 124.3 (CH), 122.9 (C), 76.6 (C), 65.7 (CH_2), 36.2 (CH_2), 35.7 (CH_2), 34.2 (C), 33.2 ($C(CH_3)_3$), 31.9 ($C(CH_3)_3$), 31.5 ($C(CH_3)_3$), 31.2 (C), 30.0 ($C(CH_3)_3$).

Crystal Data for Complex [{ONSO$^{(ethylene)}$}Hf(O-t-Bu)$_2$]. $C_{40}H_{65}NO_4SHf$; M = 834.5; triclinic; space group *P*-1; *a* = 8.9982(6) Å, *b* = 10.1098(7) Å, *c* = 28.470(2) Å, α = 91.226(4)°, β = 94.598(3)°, γ = 115.452(3)°, *V* = 2326.5(3) Å^3; *T* = 110(2) K; *Z* =

dx.doi.org/10.1021/ic501164c | Inorg. Chem. 2014, 53, 9140−9150

2; D_c = 1.214 g cm^{-3}; μ (Mo Kα) = 2.322 mm^{-1}; R_1 = 0.0517 and wR_2 = 0.1303 for 8638 reflections with $I > 2\sigma$ (I); R_1 = 0.0569 and wR_2 = 0.1328 for all 9443 unique reflections.

General Polymerization Procedure. Solution polymerization runs of *rac*-lactide were carried out at 70 and 50 °C employing 10 μmol of catalyst and 3.0 mmol of *rac*-LA in 5.0 mL of toluene (or THF). The reactions were terminated by the addition of 1 mL of methanol and the volatiles were removed under vacuum. The unreacted monomer was dissolved in methanol and the polymer was isolated by filtration, and dried under vacuum for 2 h. Homonuclear decoupled ^{1}H NMR spectrometry (500 MHz, $CDCl_3$) was employed for determining the tacticity of the PLA samples as previously described.[15,26] Molecular weights and PDI values were determined by GPC measurements according to previously published protocols.[15] Representative polymerization data using *rac*-lactide as monomer are summarized in Table 2.

■ ASSOCIATED CONTENT

Supporting Information

CCDC 990202−990206 contain the supplementary crystallographic data for this paper. This material is available free of charge via the Internet at http://pubs.acs.org.

■ AUTHOR INFORMATION

Corresponding Author

*E-mail: moshekol@post.tau.ac.il.

Notes

The authors declare no competing financial interest.

■ ACKNOWLEDGMENTS

This work was supported by the German-Israeli Foundation (GIF) and by the Israel Science Foundation. We thank "Shikun & Binui" for financial support. We thank Purac for a gift of D- and L-lactide.

■ REFERENCES

(1) (a) Miller, S. A. *ACS Macro Lett.* **2013**, *2*, 550−554. (b) Schröder, K.; Matyjaszewski, K.; Noonan, K. J.; Mathers, R. T. *Green Chem.* **2014**, *16*, 1673−1686. (c) Yates, M. R.; Barlow, C. Y. *Resour. Conserv. Recycl.* **2013**, *78*, 54−66. (d) Tschan, M. J.-L.; Brulé, E.; Haquette, P.; Thomas, C. M. *Polym. Chem.* **2012**, *3*, 836−851. (e) Williams, C. K.; Hillmyer, M. A. *Polym. Rev.* **2008**, *48*, 1−10. (f) Mecking, S. *Angew. Chem., Int. Ed.* **2004**, *43*, 1078−1085.

(2) (a) Drumright, R. E.; Gruber, P. R.; Henton, D. E. *Adv. Mater.* **2000**, *12*, 1841. (b) Auras, R.; Harte, B.; Selke, S. *Macromol. Biosci.* **2004**, 4835. (c) Vink, E. T. H.; Rábago, K. R.; Glassner, D. A.; Springs, B.; O'Connor, R. P.; Kolstand, J.; Gruber, P. R. *Macromol. Biosci.* **2004**, *4*, 551−564.

(3) Albertsson, A. C.; Varma, I. K. *Biomacromolecules* **2003**, *4*, 1466.

(4) (a) O'Keefe, B. J.; Hillmyer, M. A.; Tolman, W. B. *J. Chem. Soc., Dalton Trans.* **2001**, 2215−2224. (b) Platel, R. H.; Hodgson, L. M.; Williams, C. K. *Polym. Rev.* **2008**, *48*, 11−63. (c) Chisholm, M. H. *Pure Appl. Chem.* **2010**, *82*, 1647−1662.

(5) (a) Spassky, N.; Wisniewski, M.; Pluta, C.; Le Borgne, A. *Macromol. Chem. Phys.* **1996**, *197*, 2627−2637. (b) Zhong, Z.; Dijkstra, P. J.; Feijen, J. *J. Am. Chem. Soc.* **2003**, *125*, 11291−11298. (c) Arnold, P. A.; Buffet, J.; Blaudeck, R. P.; Sujecki, S.; Blake, A. J.; Wilson, C. *Angew. Chem., Int. Ed.* **2008**, *47*, 6033−6036. (d) Darensbourg, D. J.; Karroonnirun, O.; Wilson, S. J. *Inorg. Chem.* **2011**, *50*, 6775−6787. (e) Miyake, G. M.; Chen, E. Y.-X. *Macromolecules* **2011**, *44*, 4116−4124.

(6) (a) Wisniewski, M.; Le Borgne, A.; Spassky, N. *Macromol. Chem. Phys.* **1997**, *198*, 1227−1238. (b) Nomura, N.; Ishii, R.; Asakura, M.; Aoi, K. *J. Am. Chem. Soc.* **2002**, *124*, 5938−5939. (c) Nomura, N.; Ishii, R.; Yamamoto, Y.; Kondo, T. *Chem.—Eur. J.* **2007**, *13*, 4433−4451. (d) Pang, X.; Du, H.; Chen, X.; Wang, X.; Jing, X. *Chem.—Eur. J.* **2008**, *14*, 3126−3136. (e) Bouyahyi, M.; Grunova, E.; Marquet, N.; Kirillov, E.; Thomas, C. M.; Roisnel, T.; Carpentier, J.-F. *Organometallics* **2008**, *27*, 5815−5825. (f) Jensen, T. R.; Breyfogle, L. E.; Hillmyer, M. A.; Tolman, W. B. *Chem. Commun.* **2004**, 2504−2505. (g) Dove, A. P.; Li, H.; Pratt, R. C.; Lohmeijer, B. G. G.; Culkin, D. A.; Waymouth, R. M.; Hedrick, J. L. *Chem. Commun.* **2006**, 2881−2883.

(7) (a) Radano, C. P.; Baker, G. L.; Smith, M. R. *J. Am. Chem. Soc.* **2000**, *122*, 1552−1553. (b) Ovitt, T. M.; Coates, G. W. *J. Polym. Sci. A Polym. Chem.* **2000**, *38*, 4686−4692. (c) Ovitt, T. M.; Coates, G. W. *J. Am. Chem. Soc.* **2002**, *124*, 1316−1326.

(8) Pilone, A.; Press, K.; Goldberg, I.; Kol, M.; Mazzeo, M.; Lamberti, M. *J. Am. Chem. Soc.* **2014**, *136*, 2940−2943.

(9) Chisholm, M. H.; Patmore, N. J.; Zhou, Z. *Chem. Commun.* **2005**, 127−129.

(10) (a) Cheng, M.; Attygalle, A. B.; Lobkowsky, E. B.; Coates, G. W. *J. Am. Chem. Soc.* **1999**, *121*, 11583−11584. (b) Pietrangelo, A.; Knight, S. C.; Gupta, A. K.; Yao, L. J.; Hillmyer, M. A.; Tolman, W. B. *J. Am. Chem. Soc.* **2010**, *132*, 11649−11657. (c) Amgoune, A.; Thomas, C. M.; Roisnel, T.; Carpentier, J.-F. *Chem.—Eur. J.* **2006**, *12*, 169−179. (d) Bouyahyi, M.; Ajellal, N.; Kirillov, E.; Thomas, C. M.; Carpentier, J.-F. *Chem.—Eur. J.* **2011**, *17*, 1872−1883. (e) Liu, X.; Shang, X.; Tang, T.; Hu, N.; Pei, F.; Cui, D.; Chen, X.; Jing, X. *Organometallics* **2007**, *26*, 2747−2757. (f) Yang, S.; Du, Z.; Zhang, Y.; Shen, Q. *Chem. Commun.* **2012**, *48*, 9780−9782. (g) Chisholm, M. H.; Gallucci, J.; Phomphrai, K. *Chem. Commun.* **2003**, 48−49. (h) Cushion, M. G.; Mountford, P. *Chem. Commun.* **2011**, *47*, 2276−2278. (i) Clark, L.; Cushion, M. G.; Dyer, H. E.; Schwarz, A. D.; Duchateau, R.; Mountford, P. *Chem. Commun.* **2010**, 273−275. (j) Collins, R. A.; Unruangsri, J.; Mountford, P. *Dalton Trans.* **2013**, *42*, 759−769. (k) Romain, C.; Heinrich, B.; Bellemin Laponnaz, S.; Dagorne, S. *Chem. Commun.* **2012**, *48*, 2213−2215.

(11) (a) Ma, H.; Spaniol, T. P.; Okuda, J. *Angew. Chem., Int. Ed.* **2006**, *45*, 7818−7821. (b) Ma, H.; Spaniol, T. P.; Okuda, J. *Inorg. Chem.* **2008**, *47*, 3328−3339. (c) Kapelski, A.; Buffet, J. C.; Spaniol, T. P.; Okuda, J. *Chem.—Asian J.* **2012**, *7*, 1320−1330. (d) Chmura, A. J.; Chuck, C. J.; Davidson, M. G.; Jones, M. D.; Lunn, M. D.; Bull, S. D.; Mahon, M. F. *Angew. Chem., Int. Ed.* **2007**, *46*, 2280−2283. (e) Chmura, A. J.; Davidson, M. G.; Frankis, C. J.; Jones, M. D.; Lunn, M. D. *Chem. Commun.* **2008**, 1293−1295. (f) Zelikoff, A. L.; Kopilov, J.; Goldberg, I.; Coates, G. W.; Kol, M. *Chem. Commun.* **2009**, 6804−6806. (g) Sergeeva, E.; Kopilov, J.; Goldberg, I.; Kol, M. *Inorg. Chem.* **2010**, *49*, 3977−3979.

(12) (a) Stanford, M. J.; Dove, A. P. *Chem. Soc. Rev.* **2010**, *39*, 486−494. (b) Thomas, C. M. *Chem. Soc. Rev.* **2010**, *39*, 165−173. (c) Dijkstra, P. J.; Du, H.; Feijen. *J. Polym. Chem.* **2011**, *2*, 520−527.

(13) For a recent review, see: Sauer, A.; Kapelski, A.; Fliedel, C.; Dagorne, S.; Kol, M.; Okuda, J. *Dalton Trans.* **2013**, *42*, 9007−9023.

(14) (a) Gendler, S.; Segal, S.; Goldberg, I.; Goldschmidt, Z.; Kol, M. *Inorg. Chem.* **2006**, *45*, 4783−4790. (b) Chmura, A. J.; Davidson, M. G.; Jones, M. D.; Lunn, M. D.; Mahon, M. F.; Johnson, A. F.; Khunkamchoo, P.; Roberts, S. L.; Wong, S. S. F. *Macromolecules* **2006**, *39*, 7250−7257. (c) Schwartz, A. D.; Herbert, K. R.; Paniagua, C.; Mountford, P. *Organometallics* **2010**, *29*, 4171−4188. (d) El-Zoghbi, I.; Whitehorne, T. J. J.; Schaper, F. *Dalton Trans.* **2013**, *42*, 9376−9387. (e) Whitelaw, E. L.; Davidson, M. G.; Jones, M. D. *Chem. Commun.* **2011**, *47*, 10004−10006. (f) Buffet, J.-C.; Martin, A. N.; Kol, M.; Okuda, J. *Polym. Chem.* **2011**, *2*, 2378−2384.

(15) Stopper, A.; Okuda, J.; Kol, M. *Macromolecules* **2012**, *45*, 698−704.

(16) For a related relationship between catalyst fluxionality and PLA tacticity in *rac*-LA polymerization by yttrium phosphasalen complexes, see: Bakewell, C.; Cao, T.-P.-A.; Long, N.; Le Goff, X. F.; Auffrant, A.; Williams, C. K. *J. Am. Chem. Soc.* **2012**, *134*, 20577−20580.

(17) Yeori, A.; Gendler, S.; Groysman, S.; Goldberg, I.; Kol, M. *Inorg. Chem. Commun.* **2004**, *7*, 280−282.

(18) (a) Cohen, A.; Yeori, A.; Goldberg, I.; Kol, M. *Inorg. Chem.* **2007**, *46*, 8114−8116. (b) Cohen, A.; Goldberg, I.; Venditto, V.; Kol, M. *Eur. J. Inorg. Chem.* **2011**, 5219−5223. (c) Ishii, A.; Toda, T.; Nakata, N.; Matsuo, T. *J. Am. Chem. Soc.* **2009**, *131*, 13566−13567. (d) Nakata, N.; Toda, T.; Matsuo, T.; Ishii, A. *Inorg. Chem.* **2012**, *51*,

274−281. (e) Hu, P.; Wang, J.-Q.; Wang, F.; Jin, G.-X. *Chem.—Eur. J.* **2011**, *17*, 8576−8583.
(19) Wang, M.; Zhu, H.; Huang, D.; Jin, K.; Chen, C.; Sun, L. *J. Organomet. Chem.* **2004**, *689*, 1212−1217.
(20) Zhu, H.; Wang, M.; Ma, C.; Li, B.; Chen, C.; Sun, L. *J. Organomet. Chem.* **2005**, *690*, 3929−3936.
(21) (a) Press, K.; Cohen, A.; Goldberg, I.; Venditto, V.; Mazzeo, M.; Kol, M. *Angew. Chem., Int. Ed.* **2011**, *50*, 3591. (b) Press, K.; Venditto, V.; Goldberg, I.; Kol, M. *Dalton Trans* **2013**, *42*, 9096−9103.
(22) Bryliakov, K. C.; Talsi, E. *Eur. J. Org. Chem.* **2008**, 3369−3376.
(23) Gendler, S.; Zelikoff, A. L.; Kopilov, J.; Goldberg, I.; Kol, M. *J. Am. Chem. Soc.* **2008**, *130*, 2144−2145.
(24) Appiah, W. O.; DeGreeff, A. D.; Razidlo, D. H.; Spessard, S. J.; Pink, M., Jr.; Young, V. G.; Hofmeister, G. E. *Inorg. Chem.* **2002**, *41*, 3656−3667.
(25) Cohen, A.; Kopilov, J.; Goldberg, I.; Kol, M. *Organometallics* **2009**, *28*, 1391−1405.
(26) (a) Thakur, K. A. M.; Kean, R. T.; Hall, E. S.; Kolstad, J. J.; Lindgren, T. A.; Doscotch, M. A.; Siepmann, J. I.; Munson, E. S. *Macromolecules* **1997**, *30*, 2422−2428. (b) Chamberlain, B. M.; Cheng, M.; Moore, D. R.; Ovitt, T. M.; Lobkovsky, E. B.; Coates, G. W. *J. Am. Chem. Soc.* **2001**, *123*, 3229−3238.